DOI: 10.1002/adsc.201200067

Regio- and Stereoselective Hydroxylation of Optically Active α-Ionone Enantiomers by Engineered Cytochrome P450 BM3 Mutants

Harini Venkataraman,[a] Stephanie B. A. de Beer,[a] Daan P. Geerke,[a] Nico P. E. Vermeulen,[a] and Jan N. M. Commandeur[a,*]

[a] Division of Molecular and Computational Toxicology, LACDR, Leiden/Amsterdam Center for Drug Research, Faculty of Sciences, Vrije Universiteit, De Boelelaan 1083, 1081 HV Amsterdam, The Netherlands
Fax: (+31)-20-598-7610; e-mail: j.n.m.commandeur@vu.nl

Received: January 25, 2012; Revised: May 9, 2012; Published online: July 29, 2012

Supporting information for this article is available on the WWW under http://dx.doi.org/10.1002/adsc.201200067.

Abstract: The selective hydroxylation of an unactivated C–H bond is a crucial step in the synthesis of fine chemicals such as hydroxylated terpenoids. In the present study, the ability of 40 cytochrome P450 BM3 mutants to perform the regio- and stereoselective hydroxylation of α-ionone has been investigated. Based on their activity and selectivity to produce 3-hydroxy-α-ionone from racemic α-ionone, 6 BM3 mutants were selected. Out of these, 3 mutants (M01 A82W, M11 A82W and M11 V87I) showed high selectivity for *trans*-3-hydroxy-α-ionone formation while 3 other mutants (M11 L437N, M11 L437S and M11 L437T) formed almost equal amounts of both *cis*-3-hydroxy- and *trans*-3-hydroxy-α-ionone. Incubation with individual enantiomers showed that M11 L437N, M11 L437S and M11 L437T exhibited opposite stereoselectivity producing (3*S*,6*S*)-hydroxy-α-ionone with the (6*S*)-enantiomer and (3*S*,6*R*)-hydroxy-α-ionone with the (6*R*)-enantiomer. Thus for the first time, BM3 mutants that can selectively produce diastereomers of 3-hydroxy-α-ionone (>90% *de*), with high turnover numbers and minimal secondary metabolism, have been identified. Docking studies have been performed to rationalize the basis of the experimentally observed selectivity. In conclusion, engineered P450 BM3s are promising biocatalysts for regio- and stereoselective production of hydroxylated α-ionones for industrial applications.

Keywords: biocatalysis; cytochrome P450 BM3; diastereoselectivity; hydroxylation; α-ionone

Introduction

Ionones are a class of nor-isoprenoids which are widely used in the flavor and fragrance industry,[1] and as building blocks for many chemicals.[2] α-Ionone is one of the nor-isoprenoids which possesses characteristic organoleptic properties. Interestingly, the individual enantiomers of α-ionone possess different odors,[3] thereby making them important for the fragrance industry. The hydroxylated variants of α-ionone are also of commercial interest. For example, derivatives of 3-hydroxy-α-ionone are used as an intermediate for the total synthesis of lutein and its stereoisomers.[4] Also, 3-hydroxy-α-ionone has been shown to be a potent attractant for *B. latifrons* during pollination.[5]

The synthesis of hydroxylated variants of natural products such as terpenes and terpenoids still poses a challenge due to the formation of a variety of side products and the lack of selectivity of conventional synthetic methods.[2,6] In particular, the stereoselective hydroxylation of unactivated sp^3 C–H bonds is a challenging aspect in modern day chemistry.[7] Because enzymes can catalyze reactions with remarkable regio- and stereoselectivity under mild conditions, their use as biocatalysts for the selective production of fine chemicals has gained increased interest over the years.[8] A variety of mono-oxygenases has been used for selective oxyfunctionalization of organic substrates.[9] An important class of mono-oxygenases are the cytochrome P450s, which are heme-dependent enzymes with the ability to perform regio- and stereoselective hydroxylations of a wide range of chemicals.[10] Efforts over the last decade have been focussed on engineering P450s to obtain robust and useful biocatalysts for industrial applications.[11] Protein engineering of P450s has proved to be an excellent means to

broaden their substrate scope and specificity as well as to improve activity.[12] For example, engineered variants of cytochrome P450cam have been shown to exhibit increased regio- and stereoselectivity towards terpenes like pinene and limonene.[13]

Cytochrome P450 CYP102A1 from *Bacillus megaterium,* commonly referred to as P450 BM3, has good perspectives for the use as biocatalyst for hydroxylation reactions of industrial significance because it is the most active P450 so far identified.[14] The fact that the heme and reductase domains of P450 BM3 are fused into a single polypeptide makes the electron transfer very efficient.[15] The active site of P450 BM3 has been re-engineered to accept a broader variety of substrates including terpenoids such as ionones.[16] Although wild-type P450 BM3 exhibits a low activity towards α-ionone hydroxylation, some cytochrome P450 BM3 mutants engineered by rational design showed an increased activity. A triple mutant containing A74G F87V L188Q mutations, was shown to convert racemic α-ionone to 3-hydroxy-α-ionone (49%) in addition to a number of other products.[17] Also, BM3 mutant F87V produced a mixture of 4 oxidized products with α-ionone without any selectivity.[18]

Hydroxylation of racemic α-ionone at the C-3 position can result in the formation of four different diastereomers of 3-hydroxy-α-ionone. Individual enantiomers (6*R*)- or (6*S*)-α-ionone can be hydroxylated to (3*R*,6*R*) and (3*S*,6*R*) or (3*R*,6*S*) and (3*S*,6*S*) forms, respectively, depending on the selectivity of the reaction. Structures of the 4 possible hydroxylated diastereomers are shown in Figure 1.

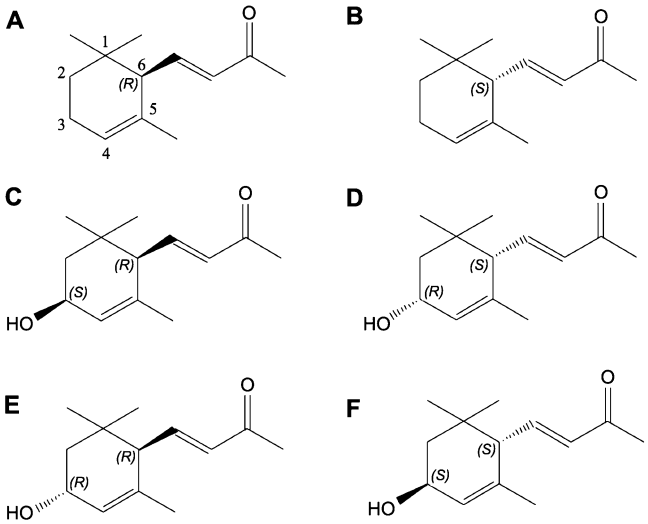

Figure 1. Structures of α-ionone enantiomers and their 3′ hydroxylated products. **A**: (*6R*)-α-ionone; **B**: (*6S*)-α-ionone; **C**: (3*S*,6*R)*-hydroxy-α-ionone; **D**: (3*R*,6*S)*-hydroxy-α-ionone; **E**: (3*R*,6*R*)-hydroxy-α-ionone; **F**: (3*S*,6*S*)-hydroxy-α-ionone. **C** and **D** are *cis* isomers while **E** and **F** are *trans* isomers (see the Supporting Information, Figure S1 for GC-MS fragmentation).

The microbial biotransformation of racemic α-ionone using different *Streptomyces* strains,[19] fungi such as *Aspergillus niger,*[20] immobilized cells of *Nicotium tabacum,*[21] and cultured cells of *Caragana chamlagu*[22] has been reported. Moreover, different bacterial P450s from *Bacillus subtillus, Sorangium cellulosum, Novaspinghobium aromaticivorans* and *Streptomyces* have been shown to hydroxylate α-ionone.[23–27] In most of the biotransformation studies of racemic α-ionone that have been reported so far, *trans*-3-hydroxy-α-ionone was found to be the main product.[19,23,25] Other studies reported the formation of 2 diastereomers of 3-hydroxy-α-ionone from racemic α-ionone hydroxylation.[17,27] However, from these studies it is not clear whether these enzymes are able to catalyze both *cis*- and *trans*-hydroxylation on each individual enantiomer, or whether they hydroxylate each enantiomer with a different diastereoselectivity.

In the present study a library of P450 BM3 mutants was evaluated for their ability to selectively produce the individual diastereomers of 3-hydroxy-α-ionone. This library was generated by a combination of site-directed mutagenesis of active site residues and random mutagenesis by error-prone PCR as described previously.[28,31,32] Thirty one mutants of the library were selected based on their proven catalytic diversity towards a variety of drugs and steroids.[28–31] Nine additional mutants were prepared by site-directed mutagenesis of active site residues A82, V87 and L437 using M01 or M11 as template, see the Supporting Information, Table S1. A detailed list of the combination of mutations present in the 40 mutants used in the present study is provided in the Supporting Information, Table S2. Because some of our P450 BM3 mutants showed both *cis*- and *trans*-hydroxy product formation with racemic α-ionone as substrate, it was decided to investigate the hydroxylation of each enantiomer individually.

In this paper, it is shown for the first time that BM3 mutants can hydroxylate individual enantiomers of α-ionone in a highly regio- and stereoselective manner and with high turnover numbers for 3 out of the 4 possible diastereomers. Thus the introduction of a hydroxy group in a single step by engineered BM3 in a highly regio- and stereoselective manner gives them good perspectives for industrial applications.

Results and Discussion

Screening of the P450 BM3 Library with Racemic α-Ionone

The goal of the initial screening was to identify P450 BM3 mutants that can produce 3-hydroxy-α-ionone with high selectivity. 40 cytochrome P450 BM3 mutants that were tested converted racemic α-ionone to

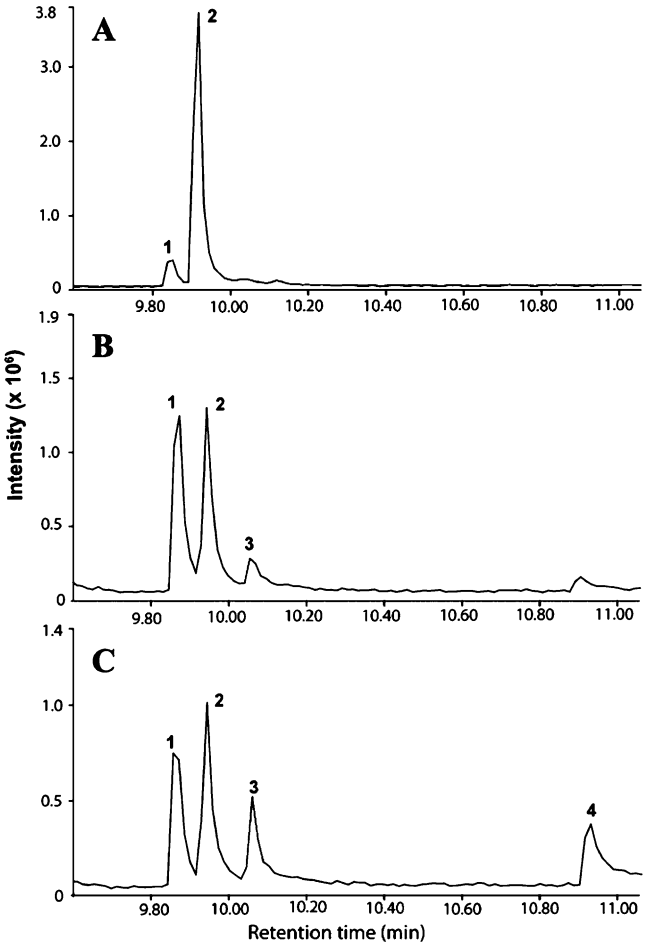

Figure 2. Gas chromatograms of biotransformation products of racemic α-ionone by (**A**) M01 A82W; (**B**) M11 L437N; (**C**) M11 A74E. Identification of the peaks: (1) *cis*-3-hydroxy-α-ionone $t_R = 9.84$; (2) *trans*-3-hydroxy-α-ionone $t_R = 9.92$; (3) 3-oxo-α-ionone $t_R = 10.02$; (4) unknown product $t_R = 10.84$.

trans-3-hydroxy- and *cis*-3-hydroxy-α-ionone with different selectivities and activities. As shown in Figure 2, three distinct product profiles were observed: mutants that converted racemic α-ionone predominantly to *trans*-3-hydroxy-α-ionone (Figure 2, **A**), mutants which produced almost equal amounts of both *cis*- and *trans*-3-hydroxy-α-ionone (Figure 2, **B**) and mutants with produced significant amounts of over-oxidation products (Figure 2, **C**). The retention times (t_R) of *cis*-3-hydroxy-α-ionone and *trans*-3-hydroxy-α-ionone were 9.84 and 9.92 min, respectively, based on the t_R of the available reference compounds.

The product profile of all the mutants tested with racemic α-ionone is shown in Figure 3. In general, most of the mutants were capable of highly regioselective C-3 hydroxylation of racemic α-ionone. C-3 is energetically the most favorable site for hydroxylation because it is an allylic methylene group. P450 BM3 mutants exhibiting high selectivity are highlighted in Figure 3. Mutants M01 A82W, M11 A82W, M11 V87I converted racemic α-ionone mainly to *trans*-3-hydroxy-α-ionone (>85% *de*), whereas mutants M11 L437N, M11 L437S and M11 L437T produced almost equal amounts of *trans*-3-hydroxy-α-ionone and *cis*-3-hydroxy-α-ionone. Consistent with a previous study,[17] wild-type P450 BM3 showed only very low activity, with a preference for *trans*-hydroxylation.

Conversion to 3-Oxo-α-ionone

Some of the mutants (M11 A74E, M11 L437T) converted racemic α-ionone to 3-oxo-α-ionone and an unidentified over-oxidation product (see the Supporting Information, Figure S4), in addition to *trans*-3-hydroxy- and *cis*-3-hydroxy-α-ionone. A representative gas chromatogram illustrating this product profile is shown in Figure 2, **C**. Incubation of purified P450 BM3 mutants with α-ionone also resulted in the formation of 3-oxo-α-ionone indicating that the secondary oxidation of alcohol to ketone is also mediated by P450 BM3. 3-Oxo-α-ionone has been recently shown to be a phagostimulant and also has commercial value because of its fragrance.[34] The exact mechanism of formation of 3-oxo-α-ionone is still to be investigated, but the formation of ketones by engineered P450 BM3 has been reported before for octane hydroxylation.[35] A possible mechanism as mentioned in these studies is the formation of a geminal diol that readily dehydrates to form the corresponding ketone group. Also, in the case of 7-hydroxy-delta8-tetrahydrocannabinol (THC) hydroxylation by hepatic microsomes from Japanese monkeys, the formation of 7-oxo-delta8-THC by a similar mechanism has been reported.[36]

Incubation with Individual Enantiomers of α-Ionone

As seen in Figure 3, from the screening of the mutants with racemic α-ionone, mutants M11 L437N, M11 L437S and M11 L437T initially appeared to be not stereoselective by producing almost equal amounts of *trans*- and *cis*-3-hydroxy-α-ionone. In order to elucidate which diastereomers are formed from each α-ionone enantiomer, these three mutants were also incubated with the individual enantiomers (6*R*)- and (6*S*)-α-ionone. All three mutants turned out to be highly stereoselective with individual enantiomers as substrate, producing (3*S*,6*S*)-hydroxy-α-ionone with the (6*S*)-enantiomer and (3*S*,6*R*)-hydroxy-α-ionone with the (6*R*)-enantiomer. Figure 4 (**A**, **B**) shows the results obtained with mutant M11 L437N. Incubation of M11 L437T with (6*R*)-α-ionone at a concentration of 500 μM resulted in the formation of about 80% of (3*S*,6*R*)-hydroxy-α-ionone,

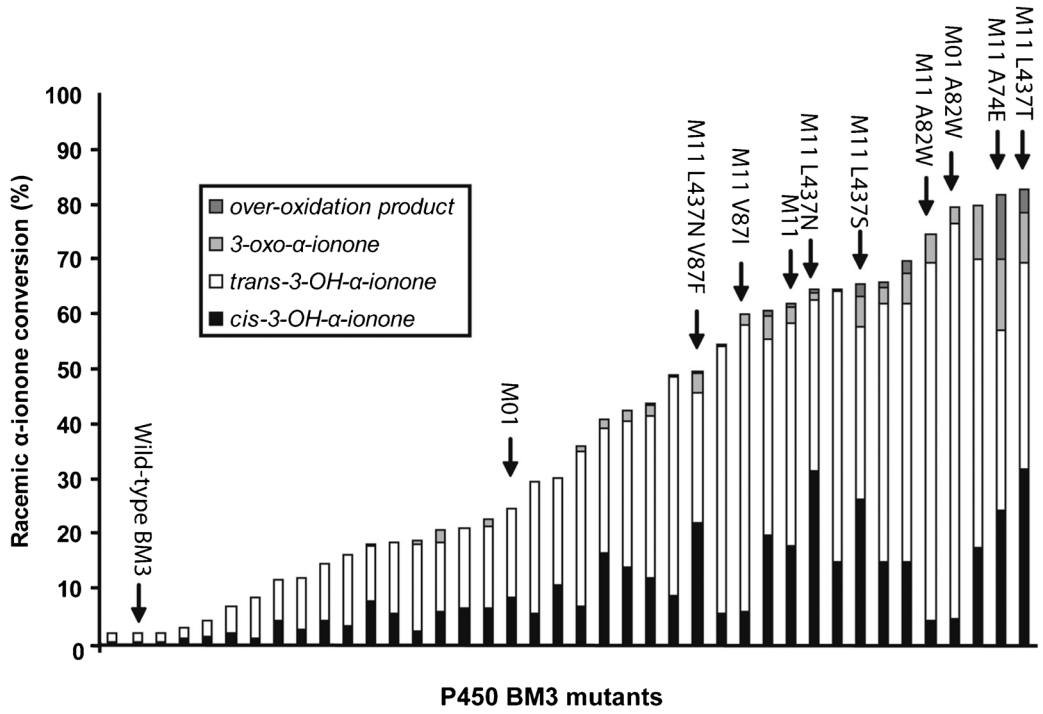

Figure 3. Product profile and conversion of racemic α-ionone by wild-type P450 BM3 and engineered variants. Conversions in % were measured from substrate consumption after 1 hour incubation of 500 μM of racemic α-ione with 200 nM of P450 BM3. Values represent averages of 2 independent experiments with less than 10% error. Product selectivity in % was calculated from gas chromatograms by integrating the product peaks. Representative P450 BM3 variants showing high selectivity towards formation of *trans*-3-α-ionone (M11 V87I, M11 A82W, M01 A82W), variants that were not selective (M11 L437N, M11 L437S, M11 L437T, M11 L437N V87F) and a variant showing high over-oxidation product formation (M11 A74E) are highlighted. Wild-type P450 BM3 and mutants M01 and M11 are also highlighted for comparison. Of the 40 mutants tested, only one variant showed $<0.5\%$ conversion (M11 V87C) and was therefore not included in Figure 3. An expanded form of Figure 3 is included in the Supporting Information (Figure S3) with all the variants labelled.

12% of (3*R*,6*R*)-hydroxy-α-ionone and 8% of 3-oxo-α-ionone as measured after 1 hour. After 12 h of incubation, α-ionone was completely converted to 3-oxo-α-ionone (see the Supporting Information, Figure S5). In contrast, 12-hour incubations of M11 L437N with α-ionone enantiomer showed only small amounts of 3-oxo-ionone. This shows that BM3 mutant M11 L437N is capable of highly selective hydroxylation with minimal formation of secondary oxidation products whereas mutant M11 L437T can result in the formation of a significant amount of 3-oxo-α-ionone.

The fact that incubations with mutant M11 showed also significant amounts (30%) of (3*R*,6*R*)-hydroxy-α-ionone with the (6*R*)-enantiomer as substrate is worthy of note, Table 1, shows that substitution L437N in mutant M11 has improved the stereoselectivity of the (*6R*)-α-ionone hydroxylation. Interestingly, L437 has been recently reported to be a 'hotspot' affecting the selectivity of terpene hydroxylation.[40] To test whether the L437N substitution also influences stereoselectivity in other M11-related mutants, the enantiomers of α-ionone were also incubated with the available combinations M11 V87F and M11 V87F L437N, and M11 A82W and M11 A82W L437N. As shown in the Supporting Information, Figure S9 A, substitution of L437N also increased the relative amount of (3*S*,6*R*)-hydroxy-α-ionone when applied to M11 V87F and M11 A82W although to a much lower extent when compared to that when applied to M11. When incubated with (6*S*)-α-ionone, the L437N substitution led to a slight increase in formation of (3*R*,6*S*)-hydroxy-α-ionone when applied to M11 V87F, whereas the substitution had no effect when applied to M11 A82W, see the Supporting Information, Figure S9B. These results confirm that the effect of a single amino acid substitution is strongly dependent on additional nearby mutations.[40, 60]

As shown in Figure 3, M01 A82W metabolized racemic α-ionone with high activity, producing mainly *trans*-3-hydroxy-α-ionone, implicating that both enantiomers of α-ionone were stereoselectively hydroxylated. This was confirmed by incubation of M01 A82W with the individual enantiomers. As shown in Figure 4 (**C**, **D**), (6*R*)-α-ionone was specifically metabolized to (3*R*,6*R*)-hydroxy-α-ionone, whereas (6*S*)-α-ionone was specifically metabolized to (3*S*,6*S*)-hydroxy-α-ionone. In both cases only mini-

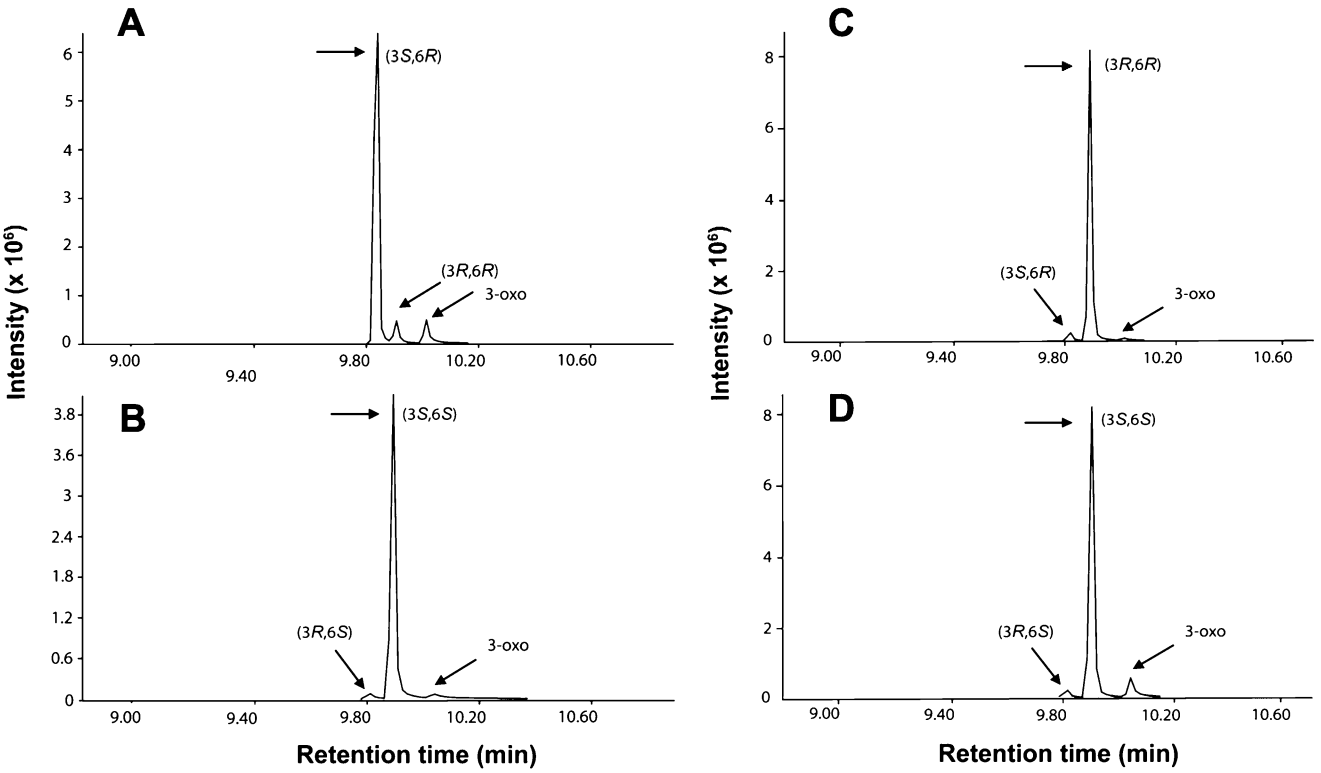

Figure 4. Representative gas chromatograms showing opposite stereoselectivity for (**A**) hydroxylation of (6*R*)-α-ionone by M11 L437N and (**B**) hydroxylation of (6*S*)-α-ionone by M11 L437N and similar stereoselectivity for (**C**) hydroxylation of (6*R*)-α-ionone by M01 A82W and (**D**) hydroxylation of (6*S*)-α-ionone by M01 A82W. In all cases, the substrate (6*R*)- or (6*S*)-α-ionone was completely oxidized to respective products.

Table 1. Stereoselective hydroxylation of (*R*)-α-ionone and (*S*)-α-ionone by wild-type P450 BM3 engineered P450 BM3 mutants.

Mutant	Substrate	Product Distribution [%][a]	Diastereomeric excess [*de* %]	Total turnover number[b]
Wild-type P450 BM3	*(R)*-α-ionone	3*R*,6*R* (53%), 3*S*,6*R* (17%), *other-oxidation** (30%)	51 (3*R*,6*R*)	–
	(S)-α-ionone	3*S*,6*S* (46%), 3*R*,6*S* (36%), *other-oxidation** (18%)	12 (3*S*,6*S*)	–
M01	*(R)*-α-ionone	3*R*,6*R* (59%), 3*S*,6*R* (30%), 3-*oxo*-α-ionone (11%)	32 (3*R*,6*R*)	–
	(S)-α-ionone	3*S*,6*S* (84%), 3*R*,6*S* (14%), 3-*oxo*-α-ionone (2%)	71 (3*S*,6*S*)	–
M11	*(R)*-α-ionone	3*R*,6*R* (35%), 3*S*,6*R* (55%), 3-*oxo*-α-ionone (10%)	22 (3*S*,6*R*)	–
	(S)-α-ionone	3*S*,6*S* (83%), 3*R*,6*S* (7%), 3-*oxo*-α-ionone (10%)	84 (3*S*,6*S*)	–
M01 A82W	*(R)*-α-ionone	3*R*,6*R* (91%), 3*S*,6*R* (5%), 3-*oxo*-α-ionone (4%)	91 (3*R*,6*R*)	3500
	(S)-α-ionone	3*S*,6*S* (95%), 3*R*,6*S* (3%), 3-*oxo*-α-ionone (2%)	95 (3*S*,6*S*)	4000
M11 L437N	*(R)*-α-ionone	3*R*,6*R* (4%), 3*S*,6*R* (90%), 3-*oxo*-α-ionone (6%)	90 (3*S*,6*R*)	3000
	(S)-α-ionone	3*S*,6*S* (91%), 3*R*,6*S* (5%), 3-*oxo*-α-ionone (4%)	91 (3*S*,6*S*)	3800

[a] Values (in %) were calculated from 2 independent experiments with not more than 10% error. For wild-type P450 BM3 the activity towards both enantiomers was too low to accurately determine the product distribution under the conditions used for other P450 BM3 mutants. Therefore, the incubations were performed at a higher enzyme concentration of 1 μM. Other-oxidation refers to the peak with $m/z = 208$ as detected on GC-MS.

[b] Total turnover numbers are reported as nmol product per nmol enzyme. The values are calculated from 2 independent experiments with ±10% error. Total turnover numbers were measured only for the enzymes which showed high diastereoselectivity towards product formation.

mal amounts of secondary oxidation products were observed. When (6*R*)-α-ionone was incubated with purified M01, significant amounts of both diastereomers were found, Table 1, indicating that mutation A82W has strongly increased stereoselectivity of hydroxylation of α-ionone.

Wild-type P450 BM3, which showed only very low activity when incubated with racemic α-ionone, showed very low diastereoselectivity, when incubated with the enantiomers of α-ionone, Table 1. When incubated with (*S*)-α-ionone, almost equal amounts of (3*S*,6*S*)- and (3*R*,6*S*)-diastereomers were found, next to significant amounts of unidentified oxidation products. When incubated with (*R*)-α-ionone, the diastereomeric excess for the (3*R*,6*R*)-diastereomer was found to be 51%.

Total Turnover Numbers for Stereoselective Hydroxylation

An optimal biocatalyst should ideally be able to catalyze the formation of the desired product in a highly selective manner (regio-, enantio- or stereo-) in combination with high catalytic turnovers and with minimal amount of secondary products.[37] Among M11 L437N, M11 L437S and M11 L437T, M11 L437N, which showed the highest diastereoselectivity (> 90%), see Figure 4, was selected for determination of the total turnover number. With respect to hydroxylation of optically active α-ionone by P450s, mutant M11 L437N is the first engineered P450 BM3 specifically producing one of the *cis*-3-hydroxy products, that is, (3*S*,6*R*), with high stereoselectivity. Additionally, among mutants that produced predominantly *trans*-3-hydroxy-α-ionone, M01 A82W was selected for incubation with individual enantiomers because it exhibited the highest diastereoselectivity as well as activity. M01 A82W catalyzed the formation of (3*S*,6*S*)-hydroxy-α-ionone and (3*R*,6*R*)-α-ionone with (6*S*)- and (6*R*)-enantiomers respectively, with remarkable selectivity.

The fact that the P450 BM3 mutants M01 A82W and M11 L437N exhibit different stereoselectivities towards hydroxylation of (*R*)-and (*S*)-enantiomers, makes them highly useful for industrial biotechnological applications. M01 A82W catalyzes the formation of (3*S*,6*S*)-hydroxy-α-ionone and (3*R*,6*R*)-hydroxy-α-ionone with turnover numbers in the range of 3500–4000, Table 1. Similarly M11 L437N can also catalyze the formation of (3*S*,6*R*)-hydroxy-α-ionone with high turnover numbers of about 3000 nmol product/nmol enzyme. These high turnover numbers indicate that these enzymes might be useful for preparative scale biosynthesis.[38]

For both M01 A82W and M11 L437N these reactions are carried out with high selectivity to the desired product with minimal formation of side products. Purified M01 A82W was used as biocatalyst with (*S*)-α-ionone (48 mg) as substrate in a volume of 250 mL to illustrate the preparative use of this engineered P450 BM3. The reaction resulted in >90% substrate conversion to produce (3*S*,6*S*)-hydroxy-α-ionone (95% *de*) under the experimental conditions mentioned. Therefore, apparently the biotransformation reaction can be scaled up without any loss of diastereoselectivity.

Binding Spectra of α-Ionone Enantiomers

The interactions of the α-ionone enantiomers with the stereoselective mutants M01 A82W and M11 L437N and their respective templates M01 and M11 were studied by spectral binding experiments. Titration of (*R*)- or (*S*)-α-ionone to solutions of purified P450 BM3 mutants in all cases resulted in typical type I difference spectra, with a peak at 390 nm and a trough at 422 nm, indicative of the conversion of heme iron from low spin to high spin. The Supporting Information, Figure S6 shows the binding spectra of both enantiomers to mutant M01 A82W. The dissociation constants obtained from these titration studies are shown in Table 2. The introduction of the A82W mutation in M01 increased binding affinity towards both enantiomers: the dissociation constant (K_d) for M01 A82W was decreased approximately 3.5-fold in the case of (*R*)-enantiomer and approximately 22-fold in the case of (*S*)-enantiomer when compared to M01. Improved affinity of hydrophobic substrates by A82W mutation in P450 BM3 has been reported previously with other substrates like fatty acids and testosterone.[29,39]

Mutation L437N in M11 also apparently increases affinity towards both enantiomers of α-ionone; dissociation constants were lowered 2.4–3.6-fold in comparison to its precursor M11, which exhibited K_d values of 17 μM and 27 μM for (*R*)-enantiomer and (*S*)-enantiomer respectively.

Wild-type P450 BM3 also showed a typical type I difference spectrum. Dissociation constants obtained were comparable to those obtained with the much more active P450 BM3 mutants, being 17.5 and 10.3 μM, respectively, for (*R*)-α-ionone and (*S*)-α-ionone.

NADPH Consumption and Product Formation

To study the coupling efficiency of the mutants and wild-type P450 BM3, the rates of NADPH oxidation and product formation were determined at 200 μM of substrate, Table 2. In case of wild-type BM3, relatively low (4–6%) coupling efficiencies were observed for

Table 2. Binding, product formation rates, NADPH oxidation rates and coupling efficiencies for hydroxylation of α-ionone enantiomers by wild-type P450 BM3, mutants M01 A82W, M11 L437N and their respective precursors M01 and M11.

	(*R*)-α-Ionone					(*S*)-α-Ionone			
	Wild-type BM3	M01	M01 A82W	M11	M11 L437N	Wild-type BM3	M01	M01 A82W	M11	M11 L437N
NADPH oxidation[a]	31 ± 5.6	260.9 ± 7.7	83 ± 4.9	128.6 ± 5.5	393 ± 21.0	29.1 ± 2.7	124 ± 16.0	221 ± 6.4	51.7 ± 3.1	210 ± 12
Product formation[b]	1.4 ± 0.6	38.4 ± 3.4	35.2 ± 2.7	58.5 ± 5.1	152 ± 8.3	1.9 ± 0.9	36.8 ± 2.0	97.8 ± 8.2	20.1 ± 1.7	85.5 ± 9.3
Coupling efficiency[c]	4.1 ± 0.5	14.8 ± 1.7	42.3 ± 1.6	45.6 ± 3.0	38.6 ± 4.3	6.5 ± 0.1	30.1 ± 4.3	44.2 ± 3.6	38.7 ± 4.2	40.7 ± 2.6
Dissociation constant[d]	17.5 ± 2.5	13.5 ± 2.1	3.8 ± 0.5	17.6 ± 3.0	7.4 ± 0.4	10.3 ± 3.1	11.6 ± 0.9	0.5 ± 0.06	27.5 ± 2.0	7.5 ± 1.1

[a] Rates of NADPH oxidation were measured over 30 s at 340 nm as nmol NADPH consumed/min/nmol enzyme. The reaction contained purified P450 BM3 (200 nM), NADPH (200 μM) and (*R*)- or (*S*)-α-ionone (200 μM) in methanol (2%) and potassium phosphate buffer (100 mM, pH 7.4).Values are calculated from 3 independent experiments and expressed as mean ± S.D.

[b] Rates of product formation were measured over 30 s as nmol total product formed/min nmol^{-1} enzyme under same conditions as above. Product distribution for M01 and M11 are summarized in Table 1.

[c] Coupling efficiency is the ratio of total amount of products to the amount of NADPH consumed expressed in percentage

[d] Dissociation constants (μM) were determined by UV-VIS spectroscopy using 1 μM enzyme in 100 mM potassium phosphate buffer, pH 7.4, titrated with a solution of either (*R*)- or (*S*)-α-ionone dissolved in methanol. All substrates produced a type I binding spectrum with a peak at 390 nm and trough at 420–422 nm.

both enantiomers: the NADPH oxidation rates upon addition of (*R*)- or (*S*)-α-ionone were found to be approximately 30 min^{-1} whereas the product formation was only about 1.5 min^{-1}. Wild-type P450 BM3 produced a mixture of 2 diastereomers of C-3 hydroxylation and an additional peak with an *m*/*z* of 208 indicating hydroxylation at another carbon with both the enantiomers. Interestingly, no over-oxidation peaks were observed with both enantiomers. (Table 1)

In case of the P450 BM3 mutants significantly higher coupling efficiencies, up to 45%, were observed when compared to wild-type P450 BM3. Introduction of mutation A82W in M01 did not significantly affect the product formation with (*R*)-α-ionone as substrate, but decreased NADPH oxidation 3-fold. The increased affinity towards (*R*)-α-ionone due to the A82W mutation in combination with a more productive binding mode therefore may explain the increased coupling efficiency.

For M11 the introduction of L437N did not increase the coupling efficiency of C-3 hydroxylation of both enantiomers, Table 2. However, the rate of both NAPDH oxidation and product formation was increased almost 3- to 4-fold. The higher affinity to M11 L437N variant and the higher stereoselectivity when compared to M11 are indicative to a different, more productive, binding mode due to the L437N mutation.

For (*S*)-α-ionone, the A82W mutation in M01 led to approximately 1.7-fold increase in rate of NADPH oxidation and 2.7-fold increase in the rate of product formation, resulting in an increased coupling efficiency of 44%. For the (*S*)-enantiomer all four variants formed predominantly *trans*-hydroxy-α-ionone with M01 A82W exhibiting the highest diastereoselectivity (95%).

The results obtained show that the tested BM3 mutants were able to catalyze the formation of 3 out of the 4 possible hydroxy diastereomers with high diasteromeric excess, Table 1. The only diastereomer that could not be produced in high enantiomeric excess was (3*S*,6*R*)-3-hydroxy-α-ionone when using (*S*)-α-ionone as substrate. Almost all BM3 mutants formed mainly (3*S*,6*S*)-3-hydroxy-α-ionone with this enantiomer as substrate, with only small amounts of (3*R*,6*S*)-3-hydroxy-α-ionone. The mutant producing the highest amounts of (3*R*,6*S*)-3-hydroxy-α-ionone was found to be M11 L437N V87F, which also showed an aselective product profile with racemic-α-ionone. This mutant produced (3*R*,6*S*)-hydroxy-α-ionone with 40% selectivity (see the Supporting Information, Figure S7). Interestingly, wild-type P450 BM3 also produced about 36% (3*R*,6*S*)-hydroxy-α-ionone but with a much lower activity compared to the BM3 mutant M11 L437N V87F. Apparently, the presence of phenylalanine at position 87 seems to increase the amount of (3*R*,6*S*)-hydroxy-α-ionone produced. Al-

though this mutant still shows only moderate selectivity for the formation of this product, it could be a good starting point to improve the stereoselectivity by directed evolution.

Docking Studies

Molecular docking studies were performed in order to rationalize the basis for the experimentally observed regio- and stereoselectivity of hydroxylation of α-ionone enantiomers. Figure 5 shows representative binding poses as observed in our docking studies on the binding of (*R*)- and (*S*)-α-ionone to M01 A82W and M11 L437N. In the case of mutant M01 A82W, the majority of obtained binding poses for both (*R*)- and (*S*)-α-ionone was found in a position suitable for C-3 hydroxylation, that is, C-3 was found within 6 Å from the heme iron catalytic center (Figure 5, **A** and **B**)[41] in line with the experimental observation that C-3 is the dominant site-of-metabolism. The introduction of 82W substantially reduces the size of the binding cavity, which results in directing the substrate closer to the heme group and in an increase in activi-

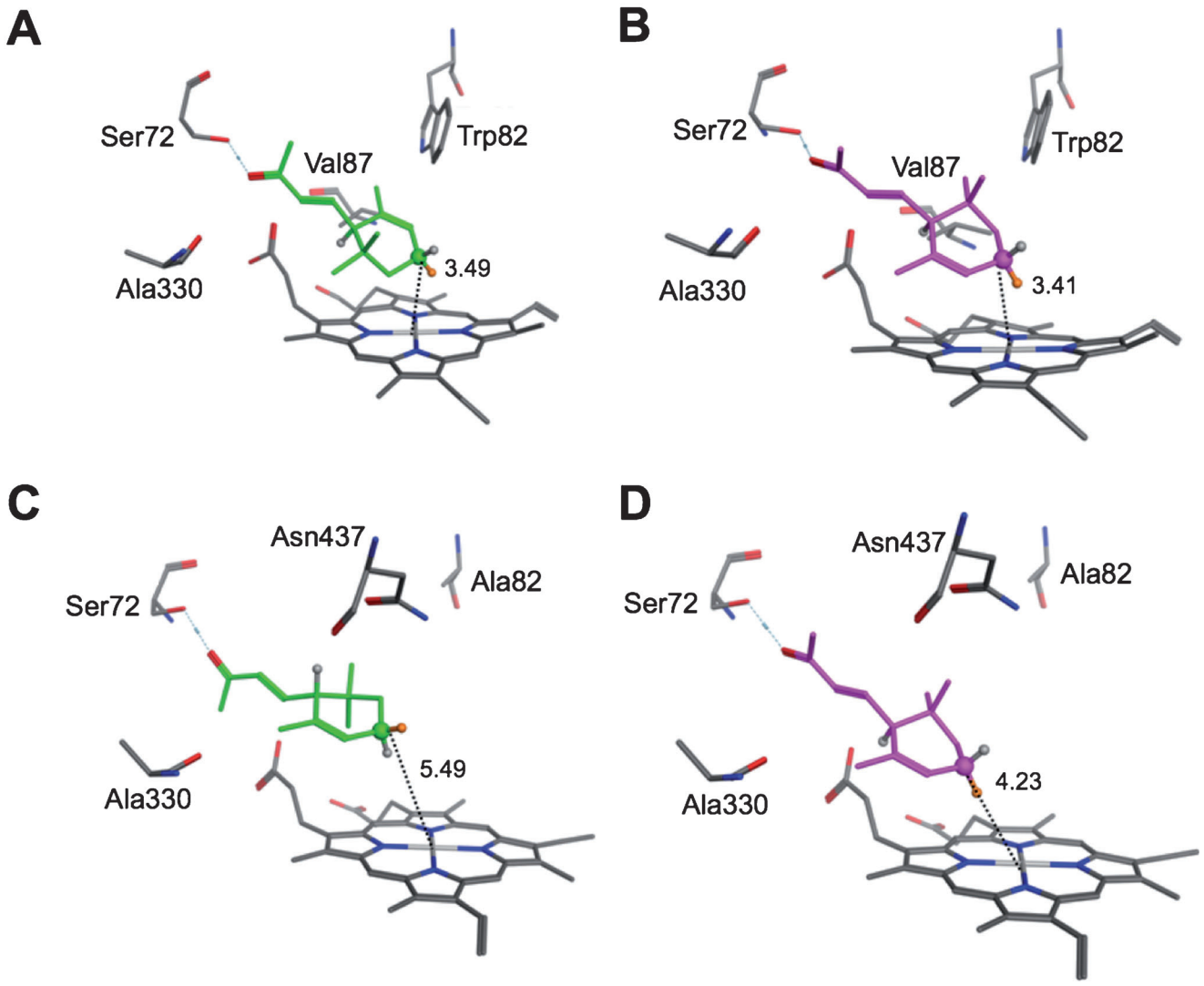

Figure 5. Binding poses of (*R*)-α-ionone (depicted in green in **A** and **C**) and of (*S*)-α-ionone (depicted in magenta in **B** and **D**) in mutant M01 A82W (**A** and **B**) and M11 L437N (**C** and **D**), as obtained from molecular docking studies. Selected amino acid residues within the binding cavity of the mutants, and the catalytic active heme moiety are depicted as well. The substrate's main site-of-metabolism (C-3) is marked by a sphere. Hydrogen atoms are omitted, except for the C-3 bound hydrogens, which are shown in small spheres; *cis*-hydrogens are depicted in grey, and *trans*-hydrogens are depicted in orange. In addition, the hydrogen atoms at the stereo-center (C-6) are explicitly shown, in small grey spheres, to highlight which stereoisomer is depicted. The thin blue line represents the hydrogen bond formed between the side-chain hydroxy moiety of the Ser72 residue, and the carbonyl oxygen of α-ionone; the dashed line represents distances (in Å) of C-3 toward the heme iron atom.

ty, in line with previous suggestions based on a study on the hydroxylation of palmitate by an A82W mutant of BM3.[39] Also among the docking poses obtained for M11 L437N in which the substrate was positioned within the catalytic cut-off, C-3 was found to be in close proximity of the heme iron atom (Figure 5, **C** and **D**). Based on the poses in which C-3 was found to be the carbon atom closest to the heme iron, the experimentally observed regioselective hydroxylation at C-3 can be explained by the formation of a hydrogen bond between the carbonyl oxygen and active site residue Ser72, which seems to anchor the ligand such that C-3 points toward the heme catalytic center, see Figure 5. Interestingly, substitution of alanine by tryptophan has been shown to affect the regioselectivity[29] and along with hydrophobic substitutions at position 72 to affect stereoselectivity of hydroxylation of larger substrates like steroids.[42] The observed anchoring of α-ionone by Ser72 is comparable to the anchoring of α-ionone by His94 upon binding to CYP109D1 as observed in a recent docking study of Khatri et al.,[25] and by Thr285 as observed in a recent docking study by Ly et al.[26] upon α-ionone binding to CYP264B1.

When docking either (*R*)- or (*S*)-α-ionone into M01 A82W, binding poses were predominantly obtained in which the C-3-bound *trans*-hydrogen is oriented toward the heme iron atom (Figure 5, **A** and **B**, respectively). Such binding poses will be referred to as "*trans*-orientated" binding poses. Experimentally, more than 90% of the products were found to be hydroxylated at the *trans* position. These findings suggest that the observed binding orientation (Figure 5, **A** and **B**) directs the stereoselectivity of the hydroxylation process, in which the substrate is oxidized by the activated iron-oxo ferryl species.[43] When docking (*S*)-α-ionone into M11 L437N, predominantly *trans*-orientated binding poses were obtained as well (Figure 5, **D**), but interestingly, only for (*R*)-α-ionone, a number of docking poses were found in which the *cis*-hydrogen was found closest to the heme iron atom (Figure 5, **C**). This offers a possible explanation for the experimental finding that hydroxylation at *cis*-position of C-3 was observed for this substrate by M11 L437N.

For M01 A82W, the (*R*)-enantiomer is oriented with the *trans*-hydrogen of C-3 closest to the heme iron atom, due to a steric conflict of the two methyl groups bound to C-1 and the bulky tryptophan side chain at the 82 position (Figure 5, **A**), whereas M11 L437N (lacking this bulky side chain) leaves more space in the active site, making it possible for the double methyl groups to point towards the residue-82 side of the cavity as seen in Figure 5, **C**. For the (*S*)-enantiomer, no such direction of the binding orientation to prevent sterical hindrance is observed, as seen in Figure 5, **B** and **D**.

The role of A82W mutation was experimentally further confirmed by incubating P450 BM3 mutant M11 L437N A82W with (*R*)-α-ionone. In line with the above discussion, the addition of A82W to M11 L437N was found to substantially decrease the stereoselectivity and *cis*-hydroxylation at C-3 position of (*R*)-α-ionone, see the Supporting Information, Figure S8. In conclusion, these docking studies support the observations that residue 82W plays an important role in the stereoselective hydroxylation of α-ionone enantiomers by M01 A82W and M11 L437N.

The presented docking studies used a wild-type BM3 crystal structure (PDB code 1BU7) as structural template for the mutants and did not explicitly account for the role of possible differences in active-site conformations and water molecule orientations, which may affect docking outcomes.[44,45] As a first exploration of the effect of active-site flexibility on our docking results, we additionally performed docking studies using another crystal structure (PDB code 1 JPZ)[46] of wild-type BM3 as structural template for the mutants. Results of these additional docking studies (data not shown) did not change the structural rationalization discussed above in terms of the orientation of the substrates' C-3 carbon atoms (with respect to the catalytical iron center) and the role played by Trp82 and Ser72 in substrate binding orientation. Currently, the structural analysis of the binding of (*R*)- and (*S*)-α-ionone to BM3 mutants such as M01 A82W and M11 L437N is extended towards a more rigorous study using molecular dynamics simulations, thereby allowing inclusion of the effects of protein plasticity[45,47] and water-mediated protein-substrate interactions,[48] to make possible a more detailed analysis of the α-ionone binding process.

Conclusions

The present study shows that individual enantiomers of α-ionone can be hydroxylated by P450 BM3 mutants with high regio- and stereoselectivity along with high turnover numbers, which makes them an attractive option for the green production of diastereomers of 3-hydroxy-α-ionone. This is the first time that such stereoselectivity of optically active α-ionone hydroxylation by P450 BM3 mutants has been reported. Moreover, the formation of (3*S*,6*R*)-hydroxy-α-ionone by M11 L437N (90% *de*) exhibits the ability of engineered P450 BM3 to produce *cis*-3-hydroxy-α-ionone. While initial docking results yield some insights into the regio- and stereoselectivity of α-ionone hydroxylation and the role played by the A82W mutation in M01 A82W, extensive free energy calculations and binding affinities of the individual enantiomers to M01 A82W and M11 L437N are needed to further understand the basis of stereoselectivity.

Experimental Section

Materials

Racemic α-ionone, enantiomers (*R*)-and (*S*)-α-ionone and the hydroxy diastereomers (3*S*,6*R*)-hydroxy-α-ionone and (3*S*,6*S*)-hydroxy-α-ionone were obtained from DSM Innovative synthesis B.V., Geleen, The Netherlands. All other chemicals were of analytical grade and purchased from Sigma unless otherwise mentioned. Restriction endonucleases were obtained from Westburg, *Pfu* polymerase and isopropyl β-D-thiogalactopyranoside (IPTG) were obtained from Fermentas.

Enzymes and Plasmids

The 31 P450 BM3 mutants used in this work were constructed as described previously.[28,31,49] Detailed information about the mutations present is tabulated in the Supporting Information, Table S2. Nine other mutants were made by site directed mutagenesis using appropriate oligonucleotides (see the Supporting Information, Table S1). In general, the mutations were introduced in the corresponding templates in pBluescript II KS(+) vector by the QuikChange mutagenesis protocol using the forward primers mentioned in the Supporting Information, Table S1. The reverse primers were exactly complementary to the forward primers. After mutagenesis, the presence of the right mutations was verified by DNA sequencing (Service XS, Leiden, The Netherlands). The whole gene was subcloned to pET28a+ vector using *Bam*HI and *Eco*RI sites and later transformed to BL21 (DE3) cells for expression.

Expression and Purification of P450 BM3 Mutants

For screening of products of racemic α-ionone hydroxylation, cytosolic fractions of the enzymes were used. Wild-type P450 BM3, mutants M01, M11, M01 A82W and M11 L437N were grown on a large scale and purified as follows: 600 mL terrific broth medium with 30 μg/mL kanamycin were inoculated with 15 mL of overnight culture. The cells were grown at 37 °C and 175 rpm until the OD_{600} reached 0.6. The protein expression was then induced by the addition of 0.6 mM IPTG. The temperature was lowered to 20 °C and 0.5 mM of heme precursor delta-aminolevulinic acid was added. Expression was allowed to proceed for 18 h. Cells were harvested by centrifugation (4600 *g*, 4 °C, 20 min) and the cell pellet was resuspended in 20 mL KPi-glycerol buffer (100 mM potassium phosphate [KPi] pH 7.4, 10% glycerol, 0.5 mM EDTA, and 0.25 mM DTT). Cells were disrupted using a French press (1000 psi, 3 repeats), and the cytosolic fraction was separated from the membrane fraction by ultracentrifugation of the lysate (120,000 *g*, 4 °C, 60 min). Then the enzymes were purified using Ni-NTA agarose (Sigma). To prevent aspecific binding, 1 mM histidine was added to the cytosolic fraction. 3 mL of Ni-NTA slurry were added to 20 mL of cytosol and the mixture was equilibrated at 4 °C for 2 h. The Ni-NTA agarose was retained in a polypropylene tube with porous disc (Pierce,Rockford,USA) and was washed 4 times with 4 mL Kpi-glycerol buffer containing 2 mM histidine. The P450 was eluted in 10 mL Kpi-glycerol containing 200 mM histidine. The histidine was subsequently removed by repeated washing with Kpi-glycerol buffer in Vivaspin 20 filtration tube (10,000 MWCO PES, Sartorius) at 4000 *g* until the histidine concentration was below 250 nM.

Incubations of P450 BM3 Mutants with α-Ionone and Analysis by GC-MS

For the biotransformation reaction, cytosolic fraction containing 200 nM of P450 BM3 mutants was incubated with 500 μM of racemic α-ionone in a final volume of 250 μL. The reaction was initiated by the addition of 25 μL NADPH regeneration system containing 5 mM NADPH, 50 mM glucose 6-phosphate and 20 units of glucose 6-phosphate dehydrogenase. The reaction was allowed to proceed for 1 hour and then stopped by placing the tubes on ice. After addition of 10 μL of 5 mM carbazole as internal standard, samples were extracted by vortexing with 2 mL of ethyl acetate for 30 sec. Subsequently samples were centrifuged at 4000 *g* for 5 min to separate phases. About 1 mL of the organic layer was then transferred to GC vials for analysis. The extracts were analyzed using a Hewlett–Packard 6890 series with ATAS Programmable Injector 2.1. Samples were separated on a DB-5 GC-column (30 m × 0.25 mm). Ionization was done by electron impact (EI) at 70 eV with the mass selective detector 5973. The injector temperature was maintained at 250 °C. The temperature program for the GC was as follows: 2 min. stationary at 60 °C, ramp at 20 °C min^{-1} to 280 °C and maintained at 280 °C for 4 min. For incubations with individual enantiomers, same conditions were used as described above.

Dissociation Constant Determination by Optical Spectroscopy

The binding of (*R*)- or (*S*)-α-ionone to wild-type P450 BM3 and mutants M01, M11, M01 A82W and M11 L437N was analyzed by optical titrations using a Shimadzu UV-2501PC spectrophotometer (Shimadzu Duisburg, Germany). The spectra for the substrate-free enzyme (1 μM) were recorded at 24 °C in 1 mL of 100 mM potassium phosphate buffer (pH 7.4) prior to addition of α-ionone enantiomers. Increasing amounts of (*R*)- or (*S*)-α-ionone dissolved in methanol were added from appropriate stocks up to a final volume of not more than 2% of the total volume of the solution. Spectra were recorded after each addition of substrate, and a difference spectrum was computed by subtraction of the starting (substrate-free) spectrum from those generated at each point in the titration. The maximum apparent absorption change induced at each point in the titration ($\Delta A_{390-422}$) was determined by subtraction of the minimum absorption value at the trough in each difference spectrum from the maximum value at the peak and these values were plotted versus corresponding concentrations of (*R*)- or (*S*)-α-ionone after correction for dilution. Data were analyzed by non-linear regression using GraphPad Prism 4 (GraphPad Sotware, San Diego, CA, USA). The spectral dissociation constants (K_D) were determined by fitting the titration binding curves to the following equation:

$$\Delta A = \frac{\Delta A_{max} \times [S]}{K_D + [S]}$$

where ΔA represents peak-to-trough absorbance difference, ΔA_{max} is the maximum absorbance difference, [*S*] is the substrate concentration and K_d is the dissociation constant of the enzyme-substrate complex. For substrate showing tight binding (K_d<1 μM), data were fitted to tight quadratic equation[50]

$$\frac{\Delta A}{\Delta A_{max}} = \frac{([E] + [S] + K_d) - \sqrt{\{([E] + [S] + K_d)^2 - 4[E] \times [S]\}}}{2[E]}$$

where ΔA represents peak-to-trough absorbance difference, ΔA_{max} is the maximum absorbance difference, [*S*] is the substrate concentration and [*E*] is the enzyme concentration.

Determination of Coupling Efficiency

NADPH oxidation rates were measured at 25 °C using a Libra S12 Biochrom UV-VIS spectrophotometer and 1 cm path length cuvettes. To measure the NADPH consumption rate, P450 BM3 (final concentration 200 nM) was mixed with 100 mM KPi buffer pH 7.4 containing 200 μM α-ionone enantiomers(*R* or *S*) in methanol (2% final) in a volume of 1 mL. The reaction was initiated by the addition of NADPH (end concentration 200 μM) and the decrease in absorption was monitored over 30 seconds. Rates were calculated based on the extinction coefficient of NAPDH $\varepsilon =$ 6,200 $M^{-1} cm^{-1}$.[51] To measure the coupling efficiency, the product formation was quantified under the same conditions. The percentage of coupling was determined as the ratio of the amount of product formed to the amount of NADPH consumed.

Determination of Total Turnover Numbers of M01 A82W and M11 L437N

200 nM of purified enzymes (M01 A82W and M11 L437N) were incubated with 1 mM of (*R*)- or (*S*)-enantiomers (2% methanol) in a total volume of 500 μL. The reaction was initiated by the addition of 50 μL NADPH regenerating system as mentioned in above. The reaction was performed in duplicate in 1.5-mL Eppendorf tubes at 24 °C for 12 h with shaking. After this incubation time, benzoxyresorufin-O-dealkylation[52] was used to check the enzyme inactivation to ensure completion of the reaction. Briefly, an aliquot of the incubation (62.5 μL) was mixed with Kpi buffer to a final volume of 125 μL. Benzoxyresorufin (25 μL) was added in the assay buffer at a final concentration of 10 μM. 100 μM of NADPH regenerating system were added to the reaction mixture and the reaction was monitored on a micro-plate reader. No increase in resorufin fluorescence was observed indicating that the enzyme was inactive. The samples were then extracted and analyzed by GC-MS as described above. Total turnover numbers were calculated as nmol of product formed per nmol enzyme by using the calibration curve of (3*S*,6*S*)-hydroxy-α-ionone ($R^2 = 0.9982$) with concentrations ranging from 0.1 mM to 1 mM.

Preparative-Scale Synthesis

Large-scale incubation was performed in a 3-L baffled flask with 250 nM of purified mutant M01 A82W, 48 mg of (*S*)-α-ionone (final concentration 1 mM) in a volume of 250 mL in 100 mM potassium phosphate buffer (pH 7.4) at 24 °C. The reaction was initiated by addition of 25 mL NADPH regenerating system. The reaction was allowed to proceed for 6 h and then the products were extracted by using ethyl acetate. The organic layer was dried over anhydrous Na_2SO_4 and analyzed by GC-MS to determine the substrate conversion and product formation.

Computational Methods

Mutants M01 A82W and M11 L437N were selected for molecular docking studies as they showed distinct stereoselectivity in C-3 hydroxylation. Molecular structures of the mutants were modeled based on chain A of the substrate-free crystal structure (PDB code 1BU7),[53] using the molecular modeling software MOE (Molecular Operating Environment).[54] Side-chains of the mutated amino acids were manually replaced using the builder tool, and polar and aromatic hydrogen atoms were added. The mutant structures were energy minimized in vacuo using the GROMOS05 biomolecular simulation package[55] and the GROMOS force field parameter set 45A4.[56] Subsequently, aliphatic hydrogen atoms were added using MOE. Molecular structures of the substrate for use in docking were manually built using the MOE program and energetically optimized using the MMFF94x force field, as implemented in MOE. Subsequently, (*R*)- and (*S*)-α-ionone were docked into the M01 A82W and M11 L437N active sites using GOLD (Genetic Optimization for Ligand Docking),[58] version 4.0, and the Chemscore scoring function.[59] The center point of the docking sphere was placed in the middle of the protein binding cavity, in between the side chain of residue 437 and the heme iron atom, from which the radius was set to 1.5 nm to define the active site of the protein. For each enantiomer, four independent docking simulations were performed. Per docking simulation, maximally 50 docked poses were retained. A maximum of 50000 operations in the GOLD genetic algorithm were performed, using a population of 100 genes. Generated binding poses for which all of the substrate's carbon atoms were positioned more than 6 Å away from the heme iron center (which is the hypothetical cut-off for catalytic activity,[41] and which is comparable to the distance of 5.6 Å between the heme iron and the C-3 atom of β-ionone in the crystal structure with PDB code 3OFU[27]) were discarded for further analysis. The remaining binding poses were visually inspected using MOE.

Acknowledgements

This work was financially supported by the Netherlands Organization for Scientific Research (NWO) within the IBOS (Integration of Biosynthesis and Organic Synthesis) program.

References

[1] P. Winterhalter, R. Rouseff, in: *Carotenoid-Derived Aroma Compounds*, Vol. 802, American Chemical Society, Washington DC, **2001**, pp 1–17.
[2] S. T. Withers, J. D. Keasling, *Appl. Microbiol. Biotechnol.* **2007**, *73*, 980–990.
[3] E. Brenna, C. Fuganti, S. Serra, P. Kraft, *Eur. J. Org. Chem.* **2002**, *33*, 967–978.
[4] F. Khachik, A.-N. Chang, *J. Org. Chem.* **2009**, *74*, 3875–3885.
[5] T. Ishida, H. Enomoto, R. Nishida, *J. Chem. Ecol.* **2008**, *34*, 1532–1535.
[6] W. A. Duetz, H. Bouwmeester, J. B. van Beilen, B. Witholt, *Appl. Microbiol. Biotechnol.* **2003**, *61*, 269–277.
[7] a) R. Fasan, *ACS Catalysis* **2012**, 647–666; b) A. T. Larsen, E. M. May, K. Auclair, *J. Am. Chem. Soc.* **2011**, *133*, 7853–7858.
[8] a) C. M. Clouthier, J. N. Pelletier, *Chem. Soc. Rev.* **2012**, *41*, 1585–1605; b) F. Hollmann, I. W. C. E. Arends, K. Buehler, A. Schallmey, B. Buhler, *Green Chem.* **2011**, *13*, 226–265.
[9] D. E. Torres Pazmino, M. Winkler, A. Glieder, M. W. Fraaije, *J. Biotechnol.* **2010**, *146*, 9–24.
[10] G. Grogan, *Curr. Opin. Chem. Biol.* **2011**, *15*, 241–248.
[11] a) E. O'Reilly, V. Kohler, S. L. Flitsch, N. J. Turner, *Chem. Commun.* **2011**, *47*, 2490–2501; b) V. B. Urlacher, M. Girhard, *Trends Biotechnol.* **2012**, *30*, 26–36.
[12] a) U. T. Bornscheuer, M. Pohl, *Curr. Opin. Chem. Biol.* **2001**, *5*, 137–143; b) D. Bottcher, U. T. Bornscheuer, *Curr. Opin. Microbiol.* **2010**, *13*, 274–282; c) P. C. Cirino, F. H. Arnold, *Curr. Opin. Chem. Biol.* **2002**, *6*, 130–135; d) S. T. Jung, R. Lauchli, F. H. Arnold, *Curr. Opin. Biotechnol.* **2011**, *22*, 809–817.
[13] a) S. G. Bell, X. Chen, R. J. Sowden, F. Xu, J. N. Williams, L. L. Wong, Z. Rao, *J. Am. Chem. Soc.* **2003**, *125*, 705–714; b) S. G. Bell, R. J. Sowden, L.-L. Wong, *Chem. Commun.* **2001**, 635–636.
[14] A. Chefson, K. Auclair, *Mol. Biosyst.* **2006**, *2*, 462–469.
[15] R. Bernhardt, *J. Biotechnol.* **2006**, *124*, 128–145.
[16] C. J. Whitehouse, S. G. Bell, L. L. Wong, *Chem. Soc. Rev.* **2012**, *41*, 1218–1260.
[17] D. Appel, S. Lutz-Wahl, P. Fischer, U. Schwaneberg, R. D. Schmid, *J. Biotechnol.* **2001**, *88*, 167–171.
[18] V. B. Urlacher, A. Makhsumkhanov, R. D. Schmid, *Appl. Microbiol. Biotechnol.* **2006**, *70*, 53–59.
[19] S. Lutz-Wahl, P. Fischer, C. Schmidt-Dannert, W. Wohlleben, B. Hauer, R. D. Schmid, *Appl. Environ. Microbiol.* **1998**, *64*, 3878–3881.
[20] Y. Yamazaki, Y. Hayashi, M. Arita, T. Hieda, Y. Mikami, *Appl. Environ. Microbiol.* **1988**, *54*, 2354–2360.
[21] Y. X. Tang, T. Suga, *Phytochemistry* **1994**, *37*, 737–740.
[22] H. Sakamaki, K.-i. Itoh, W. Chai, Y. Hayashida, S. Kitanaka, C. A. Horiuchi, *J. Mol. Catal. B: Enzym.* **2004**, *27*, 177–181.
[23] A. Celik, S. L. Flitsch, N. J. Turner, *Org. Biomol. Chem.* **2005**, *3*, 2930–2934.
[24] M. Girhard, T. Klaus, Y. Khatri, R. Bernhardt, V. B. Urlacher, *Appl. Microbiol. Biotechnol.* **2010**, *87*, 595–607.
[25] Y. Khatri, M. Girhard, A. Romankiewicz, M. Ringle, F. Hannemann, V. B. Urlacher, M. C. Hutter, R. Bernhardt, *Appl. Microbiol. Biotechnol.* **2010**, *88*, 485–495.
[26] T. T. Ly, Y. Khatri, J. Zapp, M. C. Hutter, R. Bernhardt, *Appl Microbiol Biotechnol* **2012**, *95*, 123–133.
[27] M. Ma, S. G. Bell, W. Yang, Y. Hao, N. H. Rees, M. Bartlam, W. Zhou, L. L. Wong, Z. Rao, *Chembiochem* **2011**, *12*, 88–99.
[28] M. C. Damsten, B. M. van Vugt-Lussenburg, T. Zeldenthuis, J. S. de Vlieger, J. N. M. Commandeur, N. P. E. Vermeulen, *Chem.-Biol. Interact.* **2008**, *171*, 96–107.
[29] V. Rea, A. J. Kolkman, E. Vottero, E. J. Stronks, K. A. Ampt, M. Honing, N. P. E. Vermeulen, S. S. Wijmenga, J. N. M. Commandeur, *Biochemistry* **2012**, *51*, 750–760.
[30] J. Reinen, J. S. van Leeuwen, Y. Li, L. Sun, P. D. Grootenhuis, C. J. Decker, J. Saunders, N. P. E. Vermeulen, J. N. M. Commandeur, *Drug Metab. Dispos.* **2011**, *39*, 1568–1576.
[31] E. Vottero, V. Rea, J. Lastdrager, M. Honing, N. P. E. Vermeulen, J. N. M. Commandeur, *J. Biol. Inorg. Chem.* **2011**, *16*, 899–912.
[32] B. M. A. van Vugt-Lussenburg, E. Stjernschantz, J. Lastdrager, C. Oostenbrink, N. P. E. Vermeulen, J. N. M. Commandeur, *J. Med. Chem.* **2007**, *50*, 455–461.
[33] V. Rea, S. Dragovic, J. S. Boerma, F. J. de Kanter, N. P. E. Vermeulen, J. N. M. Commandeur, *Drug Metab. Dispos.* **2011**, *39*, 2411–2420.
[34] R. Nishida, H. Enomoto, T. E. Shelly, T. Ishida, *Entomol. Exp. Appl.* **2009**, *131*, 85–92.
[35] a) E. T. Farinas, U. Schwaneberg, A. Glieder, F. H. Arnold, *Adv. Synth. Catal.* **2001**, *343*, 601–606; b) S. C. Maurer, K. Kühnel, L. A. Kaysser, S. Eiben, R. D. Schmid, V. B. Urlacher, *Adv. Synth. Catal.* **2005**, *347*, 1090–1098.
[36] T. Matsunaga, Y. Iwawaki, A. Komura, K. Watanabe, T. Kageyama, I. Yamamoto, *Biol. Pharm. Bull.* **2002**, *25*, 42–47.
[37] N. J. Turner, *Nat. Chem. Biol.* **2009**, *5*, 567–573.
[38] K. Zhang, S. El Damaty, R. Fasan, *J. Am. Chem. Soc.* **2011**, *133*, 3242–3245.
[39] W.-C. Huang, A. C. G. Westlake, J.-D. Maréchal, M. Gordon Joyce, P. C. E. Moody, G. C. K. Roberts, *J. Mol. Biol.* **2007**, *373*, 633–651.
[40] A. Seifert, M. Antonovici, B. Hauer, J. Pleiss, *ChemBioChem* **2011**, *12*, 1346–1351.
[41] E. Stjernschantz, B. M. A. van Vugt-Lussenburg, A. Bonifacio, S. B. A. de Beer, G. van der Zwan, C. Gooijer, J. N. M. Commandeur, N. P. E. Vermeulen, C. Oostenbrink, *Proteins* **2008**, *71*, 336–352.
[42] H. Venkataraman, S. B. de Beer, L. A. van Bergen, N. van Essen, D. P. Geerke, N. P. E. Vermeulen, J. N. M. Commandeur, *ChemBioChem* **2012**, *13*, 520–523.
[43] V. B. Urlacher, S. Lutz-Wahl, R. D. Schmid, *Appl. Microbiol. Biotechnol.* **2004**, *64*, 317–325.
[44] a) S. B. A. de Beer, L. A. van Bergen, K. Keijzer, V. Rea, H. Venkataraman, C. F. Guerra, F. M. Bickelhaupt, N. P. E. Vermeulen, J. N. M. Commandeur, D. P. Geerke, *Curr. Drug Metab.* **2012**, *13*, 155–166; b) S. B. A. de Beer, N. P. E. Vermeulen, C. Oostenbrink, *Curr. Top. Med. Chem.* **2010**, *10*, 55–66; c) J. Hritz, A.

de Ruiter, C. Oostenbrink, *J. Med. Chem.* **2008**, *51*, 7469–7477.
[45] F. P. Guengerich, *Proc. Natl. Acad. Sci. USA* **2006**, *103*, 13565–13566.
[46] D. C. Haines, D. R. Tomchick, M. Machius, J. A. Peterson, *Biochemistry* **2001**, *40*, 13456–13465.
[47] C. Oostenbrink, A. de Ruiter, J. Hritz, N. Vermeulen, *Curr. Drug Metab.* **2012**, *13*, 190–196.
[48] S. B. A. De Beer, N. P. E. Vermeulen, C. Oostenbrink, *Curr. Top. Med. Chem.* **2010**, *10*, 55–66.
[49] J. Reinen, S. Ferman, E. Vottero, N. P. E. Vermeulen, J. N. M. Commandeur, *J. Biomol. Screening* **2011**, *16*, 239–250.
[50] J. W. Williams, J. F. Morrison, *Methods Enzymol.* **1979**, *63*, 437–467.
[51] G. Truan, J. A. Peterson, *Arch. Biochem. Biophys.* **1998**, *349*, 53–64.
[52] B. M. A. Lussenburg, L. C. Babel, N. P. E. Vermeulen, J. N. M. Commandeur, *Anal. Biochem.* **2005**, *341*, 148–155.
[53] I. F. Sevrioukova, H. Li, H. Zhang, J. A. Peterson, T. L. Poulos, *Proc. Natl. Acad. Sci. USA* **1999**, *96*, 1863–1868.
[54] *Molecular Operating Environment (MOE)*, Montreal, Quebec, Canada: Chemical Computating Group Inc.
[55] a) W. F. van Gunsteren, S. R. Billeter, A. A. Eising, P. H. Hünenberger, P. Krüger, A. E. Mark, W. R. P. Scott, I. G. Tironi, *Biomolecular simulation: The GROMOS96 manual and user guide*, Vdf Hochschulverlag AG an der ETH Zürich, Zürich, **1996**; b) M. Christen, P. H. Hünenberger, D. Bakowies, R. Baron, R. Bürgi, D. Geerke, T. N. Heinz, M. A. Kastenholz, V. Kräutler, C. Oostenbrink, C. Peter, D. Trzesniak, W. F. van Gunsteren, *J. Comput. Chem.* **2005**, *26*, 1719–1751.
[56] R. D. Lins, P. H. Hunenberger, *J. Comput. Chem.* **2005**, *26*, 1400–1412.
[57] W. D. Cornell, P. Cieplak, C. I. Bayly, I. R. Gould, K. M. Merz, D. M. Ferguson, D. C. Spellmeyer, T. Fox, J. W. Caldwell, P. A. Kollman, *J. Am. Chem. Soc.* **1995**, *117*, 5179–5197.
[58] G. Jones, P. Willett, R. C. Glen, A. R. Leach, R. Taylor, *J. Mol. Biol.* **1997**, *267*, 727–748.
[59] M. D. Eldridge, C. W. Murray, T. R. Auton, G. V. Paolini, R. P. Mee, *J. Comput. Aid. Mol. Des.* **1997**, *11*, 425–445.
[60] A. Seifert, S. Vomund, K. Grohman, S. Kriening, V. B. Urlacher, S. Laschat, J. Pleiss, *ChemBioChem* **2009**, *10*, 853–861.

